Re-examining Electron-Fermi Relaxation in Gold Films With a Nonlinear Thermoreflectance Model

Patrick E. Hopkins
e-mail: pehopki@sandia.gov

Leslie M. Phinney

Justin R. Serrano

Sandia National Laboratories,
Albuquerque, NM 87185

In this work, we examine Fermi relaxation in 20 nm Au films with pump-probe themoreflectance using a thin film, intraband thermoreflectance model. Our results indicate that the Fermi relaxation of a perturbed electron system occurs approximately 1.10 ± 0.05 ps after absorption of a 785 nm, 185 fs laser pulse. This is in agreement with reported values from electron emission experiments but is higher than the Fermi relaxation time determined from previous thermoreflectance measurements. This discrepancy arises due to thermoreflectance modeling and elucidates the importance of the use of a proper thermoreflectance model for thermophysical property determination in pump-probe experiments. [DOI: 10.1115/1.4002778]

Keywords: Fermi relaxation, electron-electron scattering, thermoreflectance

1 Introduction

The relaxation of a perturbed electron gas into a Fermi distribution directly influences electronic scattering processes that drive electrical and thermal transport, laser induced chemical reaction and phase transitions, and optical interactions with solids. Ultrashort pulsed laser systems provide a unique measurement capability to examine the Fermi relaxation dynamics through pump-probe thermoreflectance as the transient changes in the thermoreflectance data are related to the Fermi relaxation time [1–4] and electron-phonon thermalization time [5–11] in a metal. These times, and corresponding thermal properties such as the electron-phonon coupling factor [12] G, are determined from the pump-probe thermoreflectance data by fitting rate-relaxation models, such as the two-temperature model (TTM) [13], to the experimental data. However, the key step in this process is relating the models to the thermoreflectance data. A common and traditional procedure to relate the models to the data is by assuming that the thermoreflectance response $\Delta R/R$ is directly related to the electron and phonon temperature changes through [14]

$$\frac{\Delta R}{R} = a\Delta T_e + b\Delta T_L \tag{1}$$

where a and b are the coefficients determined by scaling the electron and lattice temperature changes ΔT_e and ΔT_L, respectively, to the thermoreflectance data at various pump-probe delay times. Although this approach is valid for small perturbations in electron temperature, at high electron temperatures, the thermoreflectance response of metals can become highly nonlinear [11,15]. This nonlinearity has been shown to lead to errors in measurements of G if not properly taken into account. However, the Fermi relaxation of the electron system after short pulse laser absorption has not been as rigorously studied using pump-probe thermoreflectance as electron-phonon thermalization. Previous works by Sun et al. [3,4] used pump-probe thermoreflectance and a similar relation to Eq. (1) to show that gold exhibits a Fermi relaxation time of about 0.500 ps, far greater than the theoretical Fermi relaxation time in Au (40 fs) [16]. However, electron emission experiments conducted by Fann et al. [17,18] measured the Fermi relaxation time of a perturbed electron systems as ~1 ps, twice as high as that determined from pump-probe thermoreflectance.

In this work, we analyze pump-probe thermoreflectance data from Au films with a modified TTM and an intraband (nonlinear) thickness dependent thermoreflectance model [15]. We determine the Fermi relaxation time τ_F in Au from the thermoreflectance data as ~1.1 ps, in good agreement with the measurements from electron emission by Fann et al. [17,18], and show that not accounting for the highly nonlinear thermoreflectance in Au can cause a decrease in the prediction of τ_F and G, lending insight into the discrepancy in reported Fermi relaxation times for Au in the literature.

2 Experimental Details

Two 20 nm Au films were evaporated on a single crystalline, lightly doped Si substrate and a glass microscope cover slide (Corning 2947). We measure the transient thermoreflectance response of the two Au films with the thermoreflectance setup described in detail in Ref. [19]. In short, the laser pulses in our thermoreflectance setup emanate from a Spectra Physics Mai Tai with a repetition rate of 80 MHz, 90 fs pulse width, and a central wavelength of 785 nm. The pump pulses are further modulated with an electro-optic modulator (EOM) operating at 11 MHz and the probe pulses are time delayed using a mechanical delay stage. Due to dispersion introduced by the EOM, the pump pulses are broadened to 185 fs as measured at the sample location. The coaxial pump and probe pulses are focused onto the sample surface to a $1/e^2$ spot radius of 17 μm. The reflectance data collected with a photodiode is locked into the pump modulation frequency to give the thermoreflectance signal ($\Delta R/R$) as a function of pump-probe delay time. The raw data were adjusted to account for electronic noise [20] and thermal accumulation from the pump pulses [21] by monitoring the imaginary component of the thermoreflectance response and the pump phase. The temporal thermoreflectance responses of the two 20 nm Au thin film samples (Au/Si and Au/glass) are monitored after excitation with three different incident laser fluences, 0.7 J m^{-2}, 2.0 J m^{-2}, and 3.1 J m^{-2}. A representative thermoreflectance data set is shown in Fig. 1 for the 20 nm Au/glass sample measured with 3.1 J m^{-2} incident pump fluence. In the graphical representation of the data, we set the time of maximum thermoreflectance signal equal to $t = 0$.

3 Data Analysis

3.1 Two-Temperature Model. To quantitatively analyze the electron thermalization processes observed in the thermoreflectance data, we turn to the TTM. The two-temperature model in the thin film limit (i.e., film thickness is less than the ballistic penetration depth of the electrons ensuring minimal temperature gradient in the film) is given by [8]

$$\gamma T_e \frac{\partial T_e}{\partial t} = -G[T_e - T_L] + S(t) \tag{2}$$

Contributed by the Heat Transfer Division of ASME for publication in the JOURNAL OF HEAT TRANSFER. Manuscript received March 26, 2010; Final manuscript received June 22, 2010; published online January 14, 2011. Assoc. Editor: Pamela M. Norris.

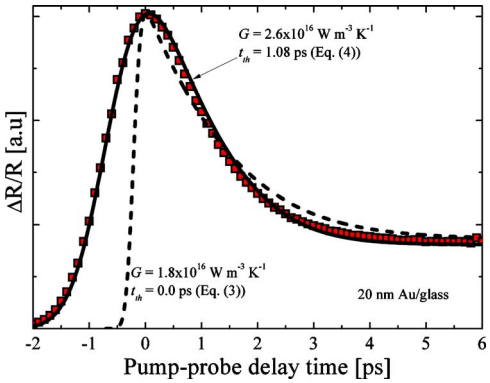

Fig. 1 Transient thermoreflectance data taken on a 20 nm Au film evaporated on a glass substrate fit with the TTM using two different source terms: (dashed line) the traditional source term (Eq. (4)) and (solid line) the source term that accounts for a delay in electron thermalization (Eq. (5)). Accounting for a delay in electron thermalization gives a much better fit of the TTM to the experimental data and yields a best fit value for *G* that is in much better agreement with previous measurements of *G* on Au.

$$C_L \frac{\partial T_L}{\partial t} = G[T_e - T_L] \tag{3}$$

where γ is the linear coefficient to the electron heat capacity, which for Au is 62.9 J m^{-3} K^{-2} [22], T_e is the electron temperature, G is the electron-phonon coupling factor, which characterizes the rate at which electrons lose energy to the vibrating lattice [12], S is the laser source term, C_L is the lattice heat capacity, and t is the time. Equations (2) and (3) are subject to the initial condition $T_e(t=0)=T_L(t=0)=T_0$ where T_0 is assumed as 300 K. The traditional source term is given by

$$S(t) = \frac{0.94F(1-R)}{dt_p} \exp\left[-2.77\left(\frac{t-2t_p}{t_p}\right)^2\right] \tag{4}$$

where F is the incident laser fluence, R is the reflectivity, d is the film thickness, and t_p is the pump pulse width (185 fs). To quantify the Fermi relaxation in the TTM formulation, we modify the standard source term to account for a delayed electron thermalization. The traditional source term in the TTM assumes that after pulse absorption, the electron system is fully thermalized. This would mean the peak reflectance would occur ~185 fs after the initial absorption process takes place. As apparent from Fig. 1, this is clearly not the case as the rise time of the fast transient is ~2 ps. Therefore, we assume the source term in the TTM is given by [23]

$$S(t) = \frac{0.94F(1-R)}{d(t_p+t_{\text{th}})} \exp\left[-2.77\left(\frac{t-2(t_p+t_{\text{th}})}{t_p+t_{\text{th}}}\right)^2\right] \tag{5}$$

where t_{th} is the delay in the electron thermalization time after pulse absorption (i.e., the Fermi relaxation time). This expression for the source term of the TTM assumes that there is a delay in thermalization beyond the pulse width. This is typically true for laser experiments using femtosecond pulses (on the order of 100 fs) interrogating metals under relatively low energy perturbations. Under energetic excitations that increase the electronic density around the Fermi level or cause a large perturbation of the electron gas from the Fermi surface, the Fermi relaxation time will decrease to that which is orders of magnitude less than the electron-phonon thermalization time and much less than the pulse width [16]. In this case, t_{th} will be negligible compared with t_p. In addition, in thicker films or bulk materials in which diffusion need be accounted for in the temperature evolution of the system, ballistic transport of the electron system can occur during pulse absorption, stretching out the depth in which the electron system equilibrates [24]. Although in this work we limit this ballistic transport phenomenon by studying Au films with thicknesses on the order of the penetration depth, to apply this delayed thermalization source term to thicker films, a correction to the depth of electronic thermalization must be employed [8].

3.2 Thermoreflectance Model. To fit the TTM to the experimental data, the change in temperature predicted by the TTM is related to the change in reflectance through an appropriate thermoreflectance model [15]. A thermoreflectance signal is a change in the baseline reflectivity of a sample surface resulting from a change in temperature of the sample. The reflectivity of a bulk material (film) at the air (vacuum)/film interface is given by

$$R = \frac{(n-1)^2 + k^2}{(n+1)^2 + k^2} \tag{6}$$

where n and k are the real (refractive index) and imaginary (extinction coefficient) parts of the complex index of refraction $\hat{n}$. The key to relating Eq. (6) to the thermoreflectance signal is knowledge of the temperature dependency of n and k for the film and substrate [25]. The refractive index and extinction coefficient are related to the complex optical dielectric function $\hat{\varepsilon}=\varepsilon_1+i\varepsilon_2$ through [26]

$$n = \frac{1}{\sqrt{2}}[(\varepsilon_1^2+\varepsilon_2^2)^{1/2}+\varepsilon_1]^{1/2} \tag{7}$$

and

$$k = \frac{1}{\sqrt{2}}[(\varepsilon_1^2+\varepsilon_2^2)^{1/2}-\varepsilon_1]^{1/2}. \tag{8}$$

Now the complex dielectric function can also be expressed as $\hat{\varepsilon}=\hat{\varepsilon}_{\text{intra}}+\hat{\varepsilon}_{\text{inter}}$, which explicitly separates the contributions due to intraband transitions (free electrons) and interband transitions (bound electrons). Since we are examining Au with 785 nm pulses, we only focus on the intraband part $\hat{\varepsilon}_{\text{intra}}$, which is described by the well known Drude model. This intraband model and its dependency on temperature is discussed in detail in Refs. [11,15].

The 20 nm thin films in this study have film thicknesses on the order of the optical penetration depth, so reflection and absorption at the film/substrate interface can cause a change in the measured reflectivity of the sample surface due to multiple reflections propagating in the film. From thin film optics, the reflectivity of a thin film on a substrate where the incident medium is air is given by [27]

$$R_f = r^* r \tag{9}$$

where

$$r = \frac{(m_{11}+\hat{n}_s m_{12})-(m_{21}+\hat{n}_s m_{22})}{(m_{11}+\hat{n}_s m_{12})+(m_{21}+\hat{n}_s m_{22})} \tag{10}$$

with $\hat{n}_s$ being the complex index of refraction of the substrate and r^* is the complex conjugate of Eq. (10). In Eq. (10), $m_{i,j}$ is the component of the characteristic thin film matrix [28] defined as

$$M = \begin{bmatrix} \cos\delta & -\frac{i}{\hat{n}_f}\sin\delta \\ -i\hat{n}_f \sin\delta & \cos\delta \end{bmatrix} \tag{11}$$

where $\delta=\omega d\hat{n}_f/c$, ω is the angular frequency of the radiation, and c is the speed of light. The temperature dependencies of the indices of refraction in this thin film reflectance model follow those of the Drude model, as previously discussed. Once Eq. (9) is determined, the intraband, thin film thermoreflectance model is given by

$$\frac{\Delta R}{R} = \frac{R_f(T_e) - R_f(T_0)}{R_f(T_0)} \tag{12}$$

With the temperature predictions from the TTM, the predicted temperature rise after short pulsed laser absorption is then converted to a thermoreflectance signal via Eq. (12) to directly compare the TTM to the experimental data.

4 Discussion

The best fit of the TTM using the thin film intraband thermoreflectance model is shown in Fig. 1. Two fits are shown: one using the TTM with the traditional source term (Eq. (4)) and the other using the source term that accounts for a delay in Fermi relaxation (Eq. (5)). The best fit electron-phonon coupling factors G using the parameters described in the text are also presented in the figure. In the graphical representation of the data, we set the time of the predicted maximum thermoreflectance signal equal to $t=0$. Using the traditional source terms results in a poor fit of the TTM to the experimental data and gives a value of G of 1.8×10^{16} W m^{-3} K^{-1}, which is low compared with previous measurements of 20 nm Au films in the low fluence limit ($2.2-4.0 \times 10^{16}$ W m^{-3} K^{-1} depending on film structure) [9,11,29,30]. Accounting for a delay in Fermi relaxation of 1.08 ps after pump pulse absorption gives a much better fit of the TTM to the experimental data. Use of this Fermi relaxation time leads to a best fit G of 2.6×10^{16} W m^{-3} K^{-1}, in much better agreement with previously measured values of G in the low fluence limit. The Fermi relaxation time was determined by fitting the TTM to the data before the peak in the data at zero delay time using t_{th} as the fitting parameter. The best fit G from the data taken with 3.1 J m^{-2}, 2.0 J m^{-2}, and 0.7 J m^{-2} incident fluences was 2.6 ± 0.3 W m^{-3} K^{-1}, 2.4 ± 0.1 W m^{-3} K^{-1}, and $2.1 \pm 0.2 \times 10^{16}$ W m^{-3} K^{-1} for the Au/glass samples and 3.2 ± 0.2 W m^{-3} K^{-1}, 2.6 ± 0.1 W m^{-3} K^{-1}, and $2.3 \pm 0.2 \times 10^{16}$ W m^{-3} K^{-1} for the Au/Si samples, respectively. The slight fluence and substrate dependency is expected due to electron scattering at the film-substrate interface during the period of electron-phonon nonequilibrium [9,10,15]. The electron thermalization time t_{th} showed no sample or fluence dependency. The average value determined from the thermoreflectance data was 1.10 ± 0.05 ps, in good agreement with the Fermi relaxation time determined from the electron emission experiments reported by Fann et al. [17,18]. However, this value for t_{th} is higher than that reported from previous thermoreflectance measurements on Au [3,4].

To understand the reason for the discrepancy between the Fermi relaxation time measurements in this work and those determined from previous thermoreflectance studies, we fit the TTM with Eq. (5) to the thermoreflectance data to determine t_{th} using the thin film intraband thermoreflectance model (Eq. (12)) and the traditionally used thermoreflectance model (Eq. (1)) (note that a comparison between a intraband thermoreflectance model and the traditionally used thermoreflectance model on determining G has been discussed previously) [11]. The Fermi relaxation time determined through the use of Eq. (12) does not exhibit a fluence dependency, which is consistent with Fermi liquid theory of hot electron relaxation; i.e., that a single particle lifetime above the Fermi level is related to the energy above the Fermi level ($t_{th} \propto (E-E_F)^{-2}$, where E is the electron energy and E_F is the Fermi energy) [31]. However, t_{th} determined through the use of Eq. (1) shows a strong fluence dependency, decreasing with increased fluence with values ranging from 0.70 ps to 1.10 ps. This is shown in Fig. 2, which plots the Fermi relaxation times as a function of incident fluence determined from the fits of the thermoreflectance data to the TTM with Eq. (5) using the traditionally used thermoreflectance model ((Eq. (1)) and the thin film intraband thermoreflectance model (Eq. (12)). In the low fluence case, Eq. (12) can be approximated by Eq. (1) since the temperature rise in the Au film is relatively small (i.e., for small temperature excursions, the thermoreflectance of a metal is approximately linear with temperature) [15], explaining the agreement of the two approaches in determining t_{th}. This further supports our finding that Fermi relaxation in Au occurs ~1.1 ps after excitation with a 785 nm (1.58 eV) laser pulse.

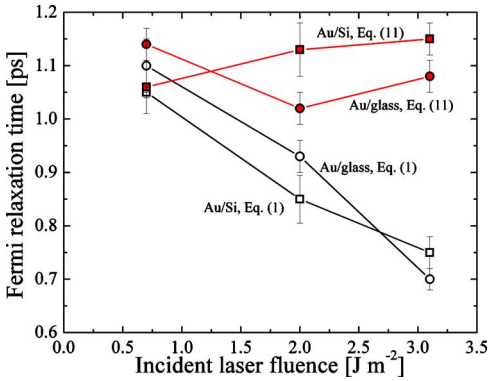

Fig. 2 Fermi relaxation times as a function of incident fluence determined from the fits of the thermoreflectance data to the TTM with Eq. (4) using the traditionally used thermoreflectance model ((Eq. (1)) and the thin film intraband thermoreflectance model (Eq. (11)). The Fermi relaxation time determined through the use of Eq. (11) does not exhibit a strong fluence dependency, which is consistent with the Fermi liquid theory of hot electron relaxation, compared with t_{th} determined through the use of Eq. (1).

5 Summary

In conclusion, we have examined electron relaxation mechanisms in 20 nm Au films with pump-probe themoreflectance using a thin film, intraband thermoreflectance model. We show that not accounting for the delayed Fermi relaxation can affect the value determined for the electron-phonon coupling factor G. Our data indicate that the Fermi relaxation of a perturbed electron system occurs approximately 1.1 ps after absorption of a 785 nm, 185 fs laser pulse. This is in good agreement with electron emission experiments [17,18] but is higher than the Fermi relaxation time determined from previous pump-probe thermoreflectance measurements on thin Au films [3,4]. This discrepancy arises due to not properly accounting for the thermoreflectance response in Au at high temperatures in the previous works, elucidating the importance of the use of a proper thermoreflectance model for thermophysical property determination in pump-probe experiments.

The relaxation and scattering mechanisms of hot electrons in solids is a critical parameter in thermal management and design of micro- and nanoscale devices. As length scales decrease and device power densities increase, the thermal resistances associated with the electronic scattering mechanisms studied in this work become increasingly dominant. For example, consider a 10 nm gold contact. The thermal resistance associated with electron-phonon scattering is described by the inverse of the electron-phonon coupling factor. Therefore, the electron-phonon resistance of the 10 nm gold contact is $\sim 5 \times 10^{-9}$ m^2 K W^{-1}. This is the equivalent resistance of 5 nm of SiO_2. With Fermi relaxation times on the same order as the electron-phonon thermalization times, as shown in this work, there will be an additional resistance due to electron thermalization mechanisms that is of the same order as the electron-phonon resistance (i.e., a few nanometers of SiO_2). Therefore, this Fermi relaxation mechanism and subsequent thermal resistance must be accounted for in the design and thermal management of next-generation devices.

Acknowledgment

P.E.H. is greatly appreciative for funding from the LDRD Program Office through the Harry S. Truman Fellowship Program. This work was performed, in part, at the Center for Integrated Nanotechnologies, a U.S. Department of Energy, Office of Basic Energy Sciences user facility; the authors would like to thank John Sullivan for assistance regarding work at the Center for Integrated Nanotechnologies. Sandia National Laboratories is a multiprogram laboratory operated by Sandia Corporation, a wholly owned subsidiary of Lockheed-Martin Corporation, for the United States Department of Energy's National Nuclear Security Administration under Contract No. DE-AC04-94AL85000.

Nomenclature

- a = coefficient related change in electron temperature to thermoreflectance, K^{-1}
- b = coefficient related change in phonon temperature to thermoreflectance, K^{-1}
- C = heat capacity, J m^{-3} K^{-1}
- c = speed of light, m s^{-1}
- d = film thickness, m
- e = exponential
- F = incident laser fluence, J m^{-2}
- G = electron-phonon coupling factor, W m^{-3} K^{-1}
- k = extinction coefficient
- m = component of the characteristic thin film matrix
- n = refractive index
- $\hat{n}$ = complex index of refraction
- R = reflectivity
- S = laser source term, W m^{-3}
- T = temperature, K
- t = time, s
- t_p = pulse width, s
- t_{th} = delay in electron thermalization after pulse absorption, s

Greek Symbols

- γ = linear coefficient to the electron heat capacity, J m^{-3} K^{-1}
- Δ = change in
- $\hat{\varepsilon}$ = complex dielectric function
- ε = dielectric function component
- τ_F = Fermi relaxation time, s
- ω = photon angular frequency, rad s^{-1}

Subscripts

- 0 = ambient
- 1 = real
- 2 = imaginary
- e = electron
- f = film
- inter = interband
- intra = intraband
- L = phonon
- s = substrate

References

[1] Groeneveld, R. H. M., Sprik, R., and Lagendijk, A., 1992, "Effect of a Nonthermal Electron Distribution on the Electron-Phonon Energy Relaxation Process in Noble Metals," Phys. Rev. B, **45**, pp. 5079–5082.
[2] Groeneveld, R. H. M., Sprik, R., and Lagendijk, A., 1995, "Femtosecond Spectroscopy of Electron-Electron and Electron-Phonon Energy Relaxation in Ag and Au," Phys. Rev. B, **51**, pp. 11433–11445.
[3] Sun, C. K., Vallee, F., Acioli, L. H., Ippen, E. P., and Fujimoto, J. G., 1993, "Femtosecond Investigation of Electron Thermalization in Gold," Phys. Rev. B, **48**, pp. 12365–12368.
[4] Sun, C. K., Vallee, F., Acioli, L. H., Ippen, E. P., and Fujimoto, J. G., 1994, "Femtosecond-Tunable Measurement of Electron Thermalization in Gold," Phys. Rev. B, **50**, pp. 15337–15348.
[5] Eesley, G. L., 1983, "Observation of Nonequilibrium Electron Heating in Copper," Phys. Rev. Lett., **51**, pp. 2140–2143.
[6] Eesley, G. L., 1986, "Generation of Nonequlibrium Electron and Lattice Temperatures in Copper by Picosecond Laser Pulses," Phys. Rev. B, **33**, pp. 2144–2151.
[7] Del Fatti, N., Voisin, C., Achermann, M., Tzortzakis, S., Christofilos, D., and Vallée, F., 2000, "Noneqilibrium Electron Dynamics in Noble Metals," Phys. Rev. B, **61**, pp. 16956–16966.
[8] Hohlfeld, J., Wellershoff, S. S., Gudde, J., Conrad, U., Jahnke, V., and Matthias, E., 2000, "Electron and Lattice Dynamics Following Optical Excitation of Metals," Chem. Phys., **251**, pp. 237–258.
[9] Hopkins, P. E., Kassebaum, J. L., and Norris, P. M., 2009, "Effects of Electron Scattering at Metal-Nonmetal Interfaces on Electron-Phonon Equilibration in Gold Films," J. Appl. Phys., **105**, p. 023710.
[10] Hopkins, P. E., and Norris, P. M., 2007, "Substrate Influence in Electron-Phonon Coupling Measurements in Thin Au Films," Appl. Surf. Sci., **253**, pp. 6289–6294.
[11] Smith, A. N., and Norris, P. M., 2001, "Influence of Intraband Transitions on the Electron Thermoreflectance Response of Metals," Appl. Phys. Lett., **78**, pp. 1240–1242.
[12] Kaganov, M. I., Lifshitz, I. M., and Tanatarov, L. V., 1957, "Relaxation Between Electrons and the Crystalline Lattice," Sov. Phys. JETP, **4**, pp. 173–178.
[13] Anisimov, S. I., Kapeliovich, B. L., and Perel'man, T. L., 1974, "Electron Emission From Metal Surfaces Exposed to Ultrashort Laser Pulses," Sov. Phys. JETP, **39**, pp. 375–377.
[14] Brorson, S. D., Kazeroonian, A., Moodera, J. S., Face, D. W., Cheng, T. K., Ippen, E. P., Dresselhaus, M. S., and Dresselhaus, G., 1990, "Femtosecond Room-Temperature Measurement of the Electron-Phonon Coupling Constant l in Metallic Superconductors," Phys. Rev. Lett., **64**, pp. 2172–2175.
[15] Hopkins, P. E., 2009, "Effects of Electron-Boundary Scattering on Changes in Thermoreflectance in Thin Metal Films Undergoing Intraband Transitions," J. Appl. Phys., **105**, p. 093517.
[16] Qiu, T. Q., and Tien, C. L., 1993, "Heat Transfer Mechanisms During Short-Pulse Laser Heating of Metals," ASME J. Heat Transfer, **115**, pp. 835–841.
[17] Fann, W. S., Storz, R., Tom, H. W. K., and Bokor, J., 1992, "Direct Measurement of Nonequilibrium Electron-Energy Distributions in Subpicosecond Laser-Heated Gold Films," Phys. Rev. Lett., **68**, pp. 2834–2837.
[18] Fann, W. S., Storz, R., Tom, H. W. K., and Bokor, J., 1992, "Electron Thermalization in Gold," Phys. Rev. B, **46**, pp. 13592–13595.
[19] Hopkins, P. E., Serrano, J. R., Phinney, L. M., Kearney, S. P., Grasser, T. W., and Harris, C. T., 2010, "Criteria for Cross-Plane Dominated Thermal Transport in Multilayer Thin Film Systems During Modulated Laser Heating," ASME J. Heat Transfer, **132**, p. 081302.
[20] Schmidt, A. J., Cheaito, R., and Chiesa, M., 2009, "A Frequency-Domain Thermoreflectance Method for the Characterization of Thermal Properties," Rev. Sci. Instrum., **80**, p. 094901.
[21] Stevens, R. J., Smith, A. N., and Norris, P. M., 2006, "Signal Analysis and Characterization of Experimental Setup for the Transient Thermoreflectance Technique," Rev. Sci. Instrum., **77**, p. 084901.
[22] Kittel, C., 1996, *Introduction to Solid State Physics*, Wiley, New York.
[23] Chen, J. K., Tzou, D. Y., and Beraun, J. E., 2006, "A Semiclassical Two-Temperature Model for Ultrafast Laser Heating," Int. J. Heat Mass Transfer, **49**, pp. 307–316.
[24] Brorson, S. D., Fujimoto, J. G., and Ippen, E. P., 1987, "Femtosecond Electronic Heat-Transport Dynamics in Thin Gold Films," Phys. Rev. Lett., **59**, pp. 1962–1965.
[25] Hopkins, P. E., 2010, "Influence of Electron-Boundary Scattering on Thermoreflectance Calculations After Intra- and Interband Transitions Induced by Short-Pulsed Laser Absorption," Phys. Rev. B, **81**, pp. 035413.
[26] Hummel, R., 2001, *Electronic Properties of Materials*, Springer, New York.
[27] Abeles, F., 1967, "Advanced Optical Techniques," *Optics of Thin Films*, North-Holland, Amsterdam.
[28] Macleod, H. A., 2001, *Thin-Film Optical Filters*, Institute of Physics, Bristol, UK.
[29] Hostetler, J. L., Smith, A. N., Czajkowsky, D. M., and Norris, P. M., 1999, "Measurement of the Electron-Phonon Coupling Factor Dependence on Film Thickness and Grain Size in Au, Cr, and Al," Appl. Opt., **38**, pp. 3614–3620.
[30] Qiu, T. Q., and Tien, C. L., 1993, "Size Effects on nonequilibrium Laser Heating of Metal Films," ASME J. Heat Transfer, **115**, pp. 842–847.
[31] Pines, D., and Nozieres, P., 1999, *The Theory of Quantum Liquids*, Benjamin-Cummings, New York.